Journal of Materials Chemistry B

Accepted Manuscript

ROYAL SOCIETY OF CHEMISTRY

www.rsc.org/materialsB

Journal Name

RSCPublishing

ARTICLE

3D Hydrogels with High Resolution Fabricated by Two-photon Polymerization with Sensitive Water Soluble Initiator

Cite this: DOI: 10.1039/x0xx00000x

Received 00th January 2012,
Accepted 00th January 2012

DOI: 10.1039/x0xx00000x

www.rsc.org/

Jinfeng Xing*[a], Ling Liu[a], Xiaoyan Song[a], Yuanyuan Zhao[b], Ling Zhang[a], Xianzi Dong[b], Feng Jin[b], Meiling Zheng*[b], and Xuanming Duan*[b,c]

Hydrogels with precise 3D configuration (3D hydrogels) is crucial for biomedical applications such as tissue engineering and drug delivery, which demand for the improvement of the spatial resolution on both the microscopic and the nanometric scale. In this study, a water soluble two-photon polymerization (TPP) initiator (WI) with high initiating efficiency was prepared by using poloxamer (PF127) to encapsulate 2, 7-bis(2-(4-pentaneoxy-phenyl)-vinyl)anthraquinone via hydrophilic-hydrophobic assembly. The threshold energy for WI was 6.29 mW at a linear scanning speed of 10 μm/s, which was much lower than those reported previously. The lateral spatial resolution of 92 nm was achieved as the resolution breakthrough of 3D hydrogels. Finally, the microstructure with high accuracy simulating the morphology of adenovirus was fabricated at the laser power close to the threshold energy of TPP, further demonstrating the ultrahigh resolution of 3D hydrogels.

Introduction

Hydrogels are commonly referred to as polymeric materials with water contents similar to that of soft tissues.[1, 2] Hydrogels with precise three dimensional configuration (3D hydrogels) are crucial for those biomedical applications such as tissue engineering and drug delivery.[3-5] Conventional microfabrication technologies such as electron beam lithography,[6, 7] interference lithography,[8] and nanoimprint lithography[9] have been developed to prepare 2D and 3D microstructures. Unlike other 3D printing technologies, two-photon polymerization (TPP) microfabrication (TPPM) induced by a near-infrared femtosecond laser can fabricate arbitrary and ultraprecise 3D microstructures with high resolution not only on the microscopic scale but also on the nanoscale.[10-13] Thus, TPP microfabrication is an promising 3D printing technology to fabricate 3D hydrogels with a precise 3D configuration of high spatial resolution.[13]

Watanabe et al. fabricated a photoresponsive 3D hydrogel of cantilever that deforms under illumination.[14] Ovsianikov et al. reported several different 3D hydrogels used for 3D cell scaffolds.[15, 16] They produced highly porous 3D hydrogel scaffolds by TPP of poly(ethylene glycol) diacrylate (PEGda) with a molecular weight of 742 Da and seeded them with cells by means of laser-induced forward transfer (LIFT). Torgersen et al. prepared 3D hydrogels as a toolbox for mimicking the extracellular matrix.[2] Using a highly efficient water soluble initiator, 1,4-bis(4-(N,N-bis(6-(N,N,N-trimethylammonium)hexyl)amino)-styryl)-2,5-dimethoxybenzene tetraiodide, photocurable resin composed of 700 Da PEGda was processed with high precision and reproducibility at a writing speed of 10 μm s^{-1}.[15, 17] In our previous work, Xiong et al. used an asymmetric TPP microfabrication method to fabricate the size and shape controlled stimuli-responsive asymmetric hydrogel microcantilevers.[18] In another work, Xing et al. fabricated 3D hydrogels of woodpile structure similar to cell scaffolds with 700 Da PEGda as a monomer and a crosslinker by using an average power of 9.7 mW at a scanning speed of 30 μm s^{-1}. The laser threshold energy for the fabrication of 3D hydrogels was

dramatically decreased and the resolution was largely improved. Finally, lateral spatial resolution (LSR) of 3D hydrogels reached 200 nm.[19]

The resolution is a key parameter for 3D hydrogels to precisely simulate the native 3D environment in which the cells reside and the drug is controlled to release with optimal temporal and spatial distribution *in vitro and in vivo*.[3, 20] Since 3D hydrogels are easily deformed due to the high water content, the improvement of their spatial resolution faces a big challenge.[21] Several strategies have been developed to improve the resolution of TPP.[10, 22-26] Undoubtedly, it is a convenient and direct method to use a highly sensitive initiator to improve the resolution of 3D hydrogels fabricated by TPP microfabrication.[10, 23]

In this study, a facile assembly method was firstly used to prepare a water soluble initiator by using poloxamer (PF127) to encapsulate 2, 7-bis(2-(4-pentaneoxy-phenyl)-vinyl)-anthraquinone via hydrophilic-hydrophobic assembly. The polymerization threshold power was decreased to 6.29 mW and the LSR was improved to 92 nm. Moreover, 3D hydrogels simulating the morphology of adenovirus were prepared.

Experimental

Materials

2, 7-bis(2-(4-pentaneoxy-phenyl)-vinyl)-anthraquinone (N) was prepared according to the reference.[27] N-Bromosuccinimide (NBS), benzoyl peroxide (BPO), triphenylphosphine (PPh_3) and all of the solvent were obtained from Jiangtian Chemical Reagent Company. 4-methylphthalic anhydride was purchased from TCI (Shanghai) Chemical Reagent Company. P-dimethylaminobenzaldehyde (PDAB) was purchased from Aladdin Chemical Reagent Company. Poloxamer (Pluronic F127), poly (ethylene glycol) diacrylate (PEGda, M_n=700) and 2-benzyl-2-(dimethylamino)-4'-morpholinobutyrophenone were purchased from Sigma-Aldrich Reagent Company. 3-Methacryloxypropyltrimethoxysilane (KH-570) was purchased from Nanjing Chuangshi Chemical Co., Ltd.

Preparation of water soluble initiator (WI)

The self-assembly experiment was performed at different molar ratio of Pluronic F127/N (1:1). In detail, poloxamers (1065 mg, 0.085 mmol) were dissolved in water (50 mL) and N (12.5 mg, 0.021 mmol) was dissolved in 25 mL of tetrahydrofuran (THF) at room temperature. The specific self-assembly experiments were taken as follows: The solution of poloxamers (2.5 mL) in distilled water (22.5 mL) were added to round bottom flask, and then N (5 mL) was added slowly and kept stirring at 40 °C for 24 h. After THF volatilized completely, the sample was prepared by freezed-dried technique. Finally, the lyophilized powder of WI was obtained.

Measurement of UV-Vis absorption and fluorescence spectra

UV-Vis spectra were measured with a Hitachi U-3900 spectrophotometer. One-photon fluorescence spectra (OPFL) were measured with Hitachi F-4600 spectrometer using a Xenon lamp as a light source with the emission and excitation slit of 5 nm and 10 nm, respectively.

Characterization of ^{1}HNMR spectroscopy

In order to demonstrate the molecular structure of N, and successful assemble of N and poloxamer. ^{1}HNMR were tested by using Varian Jemini-300 with trimethylsilane (TMS) as an internal standard and reference for chemical shifts.

Measurement of fluorescence quantum yield

The fluorescence quantum yield (Φ) of samples in solutions were recorded by using coumarin 307 (Φ=0.58) in acetonitrile as a reference standard. N and WI were dissolved in $CHCl_3$ and deionized H_2O, respectively. Φ was obtained by the following equation.[28, 29]

$$\Phi_s = \Phi_r \left[\frac{A_r(\lambda_r)}{A_s(\lambda_s)}\right]\left[\frac{I_r(\lambda_r)}{I_s(\lambda_s)}\right]\left[\frac{n_s}{n_r}\right]^2\left[\frac{F_s}{F_r}\right]$$

Where Φ is the fluorescence quantum yield, n is the refractive index, $I(\lambda)$ is the relative intensity of exciting light at wavelength λ, $A(\lambda)$ is the absorbance of solution at the exciting wavelength λ, and F is the integrated area under the emission spectrum. Subscripts s and r refer to the sample and reference solution, respectively.

Measurement of two-photon absorption cross-section

Two-photon absorption (TPA) cross-section (δ_{TPA}) was measured by using the two-photon induced fluorescence[30] method with the standard fluorescein in NaOH aqueous solution (pH=13) at the concentration of 1.0×10^{-4} M according to the reference.[31] Two-photon fluorescence spectra were recorded using SD2000 spectrometer (Ocean Optics), excited by a femtosecond laser (Mai Tai, Spectra-Physics, Fremont, CA) with a pulse width of 100 fs and repetition rate of 80 MHz in the wavelength range of 710-890 nm. It is assumed that the quantum efficiencies after two-photon excitation are the same as those after one-photon excitation. δ_{TPA} was calculated by the following equation.[28, 29]

$$\delta_s = \delta_r \frac{C_r}{C_s}\frac{n_r}{n_s}\frac{F_s}{F_r}\frac{\Phi_r}{\Phi_s}$$

Where δ is the TPA cross section, C and n are the concentration and refractive index of the sample solution, F is the integrated area obtained from the TPEF spectrum. Subscripts s and r refer to the sample and reference solution, respectively.

Two-photon polymerization processing

In this process, we used near infrared Ti:Sapphire femtosecond laser beam (120 fs, 80 MHz, 780 nm) was used to fabricate 3D hydrogels. The photoresist is composed of poly(ethylene glycol) diacrylate (PEGda)[2] as monomer (780 mg), lyophilized WI as initiator, and 2-benzyl-2-(dimethylamino)-4'-morpholinobutyrophenone as photosensitizer. The contents of monomer, initiator and photosensitizer are 780 mg, 0.5 mL (74

mg/mL aqueous solution) and 0.5 mL (30 mg/mL in DMSO), respectively. The photoresist was prepared by mixing three solutions in a glass bottle and stirred for 5 minutes before TPP fabrication. The cleaned glass slides were dipped in KH-570 toluene solution (KH-570/toluene solution = 5 wt %) overnight to guarantee the hydrophilicity of the glass surface.[32] The photoresist was dropped on the modified glass substrate above the xyz-step motorized stage (P-563.3 CL, Physik Instrument) controlled by a computer. The laser beam was focused tightly by a 100 × oil immersion objective lens with a high numerical aperture (NA=1.45, Olympus). The focal point was focused on the liquid resin. Finally, the unpolymerized resin was developed by ethanol. The SEM images of 3D structures were observed with a field-emission scanning electron microscope (SEM, Hitachi S-4800). Before SEM measurement, the sample was coated with a thin gold film to ensure images with high definition and protect from possible damage by electrons.

Results and Discussion

Linear optical properties

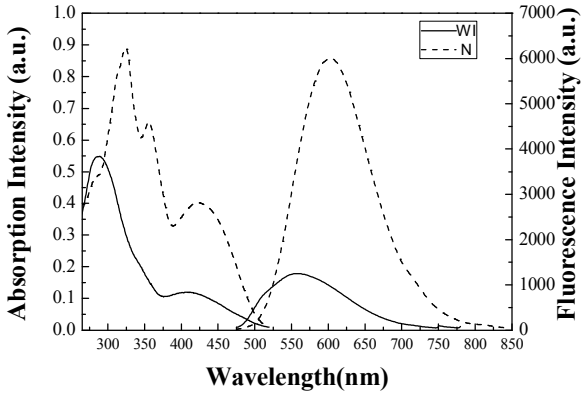

Fig. 1 Normalized UV-Vis and fluorescence spectra of WI (solid line), N (dashed line). The solvents were H_2O and THF for WI and N, respectively. The excitation wavelength for fluorescence measurement is 425 nm.

The UV-Vis absorption and fluorescence spectra of N and WI are shown in Fig. 1, in which N in THF has two main absorption peaks at 318 nm and 423 nm. As shown in Fig. 1, the absorption peak at 318 nm is assigned to the typical π-π* transition corresponding to the localized excitation state.[33] The intramolecular charge transfer (ICT) singlet state mainly deactivates through a nonradiative decay to the ICT triplet state via intersystem crossing.[27] The absorption peak at 423 nm corresponds to electronic transition from the ground state to ICT state. The OPFL of N with a single peak localizing at a wavelength of 602 nm was obtained with the excitation wavelength of 425 nm (Fig. 1), indicating that the fluorescence emission occurs from the local excited state. The absorption maximum of WI in water is 285 nm with a 33 nm hypsochromic shift compared with N due to the decreasing of the polarity of the microenvironment around N.[34] Another possible reason is that O-H/O and C-H/O hydrogen bonds formed between poloxamer and N, resulting in the electron redistribution and the increase of the stability of N simultaneously.[35] The OPFL of WI in water appears at the wavelength of 557 nm, which has a hypsochromic shift compared with that of N.

NMR studies of N and assemblies

The ^{1}H NMR spectra of N in $CDCl_3$, PF127 in D_2O and WI in D_2O are shown in Fig. 2. Two characteristic peaks at chemical shifts of 1.44 ppm (CH_3-CH_2-CH_2-CH_2-CH_2-) and 1.78 ppm (CH_3-$(CH_2)_2$-CH_2-CH_2-) are attributed to methylene protons corresponding to the alkyl chain of N. Other characteristic peaks at chemical shift of 8 ppm approximately correspond to phenyl protons of N (Fig. 2a). PF127 as amphiphilic copolymer in water could self-assemble into micelles with hydrophobic core and hydrophilic shell. When N assembles with PF127, N should be encapsulated into hydrophobic core. To confirm whether N can be encapsulated into PF127 completely, ^{1}H NMR spectra of WI in D_2O was measured. As shown in Fig. 2b and 2c, it is found that only characteristic peaks of PF127 appear, demonstrating that N was completely encapsulated into hydrophobic core of PF127.

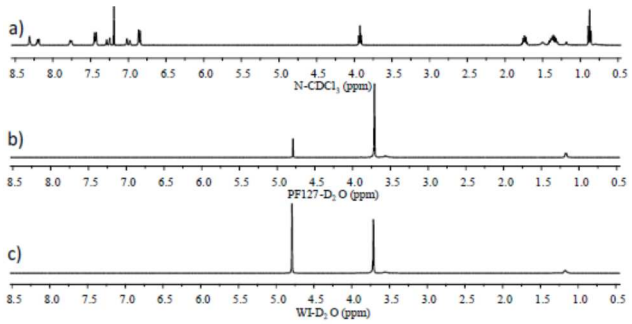

Fig. 2 (a), (b) and (c) is the ^{1}H NMR spectra (500 MHz) of N in $CDCl_3$, PF127 in D_2O, and WI in D_2O, respectively.

Nonlinear optical properties

The TPA nonlinear relationship and δ_{TPA} of N and WI are shown in Fig. 3a and 3b, respectively. In theory, the absorption of N and WI is a TPA process in condition that the slope (K) of the relationship between logarithm of the fluorescent integral area (F) and laser energy (P) of N and WI is around 2. As shown in Fig. 3a and 3b, K of N and WI is 2.02 and 1.81, respectively, indicating that the absorption of N and WI is a TPA process. The maximum of δ_{TPA} for N and WI is around 600 GM and 260 GM at the wavelength of 820 nm and 760 nm, respectively. In aqueous medium, the δ_{TPA} of WI is around 200 GM at 780 nm which is much larger compared with those commercial initiators and most of water soluble TPA materials reported with a low δ_{TPA} less than 100 GM.[30, 31] Compared to N, the δ_{TPA} of WI is smaller. The reason is that there are many N molecules aggregated in each micelle. When WI was excited by the laser of 780 nm, only a part of N in micelle could be excited.[31]

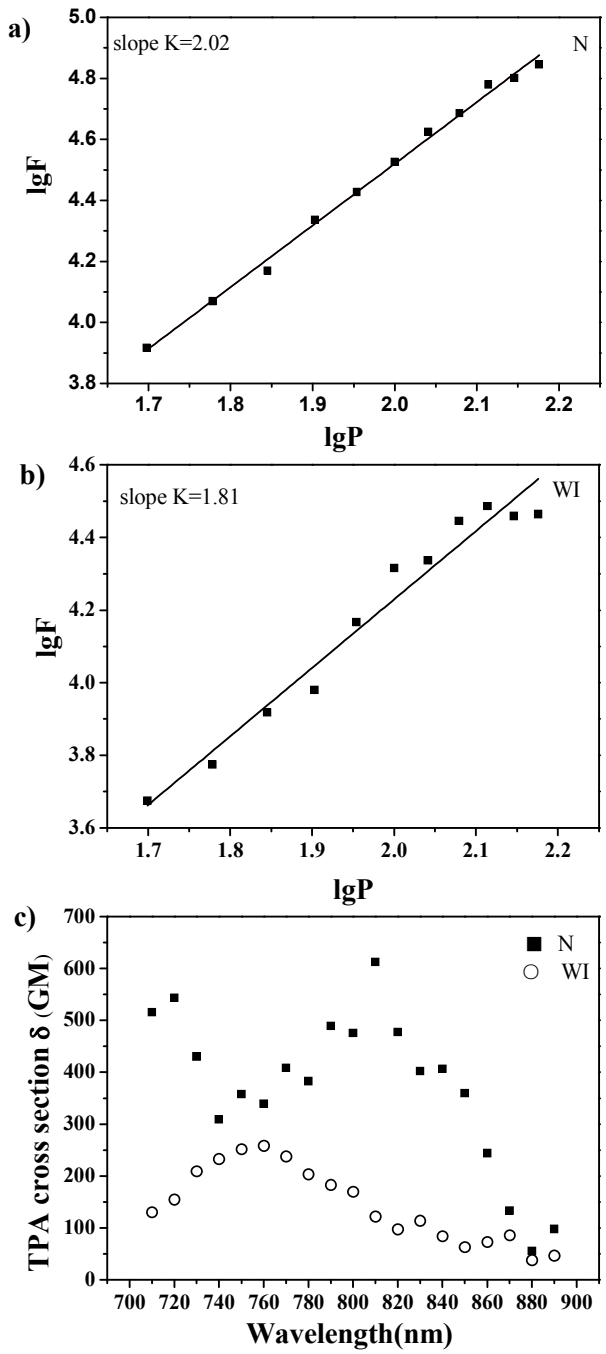

Fig. 3 The nonlinear relationship between two-photon fluorescence and the laser power for N (a) and WI (b), and δ_{TPA} of N and WI (c) at wavelength in the range of 710-890 nm. N and WI are dissolved in $CHCl_3$ and H_2O, respectively.

Investigation of the lateral spatial resolution for 3D hydrogels

The resolution is a key parameter for 3D hydrogels to precisely simulate the native 3D environment in which the cells reside and the drug is controlled to release with optimal temporal and spatial distribution *in vitro and in vivo*.[3, 20] The resolution of 3D hydrogels depends on the laser power and exposure time of TPP microfabrication. The threshold energy of TPP microfabrication is crucial for the resolution of 3D hydrogels. The resolution of 3D hydrogels can be improved by decreasing the threshold energy of TPP microfabrication. In this study, the threshold energy for WI at a linear scanning speed of 10 μm s^{-1} was 6.29 mW, which was much lower than those reported previously.[19, 36, 37] In this case, it is possible to achieve higher resolution of 3D hydrogels when the laser power of TPP is close to 6.29 mW compared with the previously reported resolution of 3D hydrogels.[19] On one hand, the high efficiency of WI can be attributed to the excellent solubility of WI in water. On the other hand, the number of hydroxyl group as radical quencher in PF127 is less than that of cyclodextrin used in our previous work.[19] To investigate the possibility of further improvement of LSR, the relationship between the LSR and laser power at a linear scanning speed of 10 μm s^{-1} was confirmed by tuning the laser power from 11.09 mW to 6.29 mW (Fig. 4). When the laser power was reduced to 6.8 mW, a 92 nm of LSR was achieved. To our knowledge, this is the first time that LSR of hydrogel was improved to a value less than 100 nm, which is much better than 200 nm, the latest resolution of LSR for 3D hydrogels.[19]

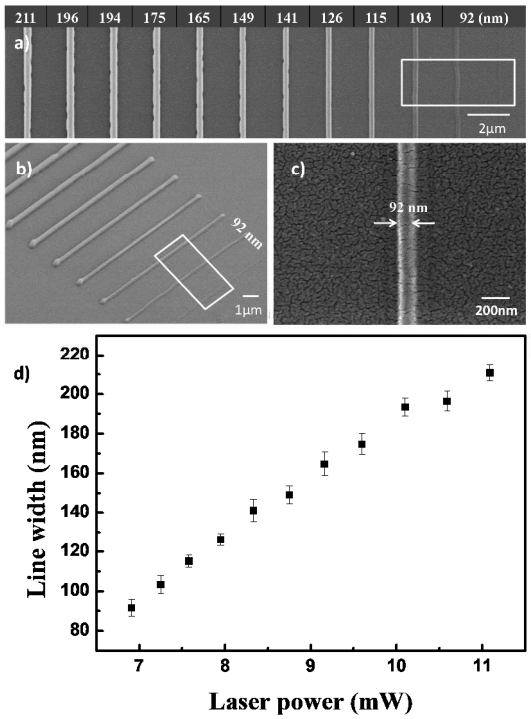

Fig. 4 (a) Top view and (b) side view of the SEM images of lines fabricated at the constant scanning speed of 10 μm s^{-1} with the laser power ranging from 11.09 to 6.29 mW. The selected area shown in (a) and (b) represent the lines fabricated with laser power close to the laser threshold. (c) The magnified SEM image of the line of 92 nm. (d) The relationship of laser power and line width corresponding to (a).

Two-photon polymerization microfabrication of 3D hydrogels simulating the morphology of adenovirus

The biomedical applications of 3D hydrogels such as tissue engineering and drug delivery put forward rigorous requirements on the processing accuracy of TPP

microfabrication, including the dimensional accuracy, shape accuracy and surface roughness. LSR is important for the processing accuracy of TPP microfabrication. High LSR benefits to improve the processing accuracy of TPP microfabrication. As mentioned above, a 92 nm of LSR was achieved, indicating that microstructure with high accuracy is able to be fabricated when the laser power is close to the threshold energy. To demonstrate the fabrication capability, we have designed a model of adenovirus by using 3D Max software. During the TPP fabrication, the computer controlled the movement of stage according to the preprogrammed pattern with a scanning speed of 110 μm/s. The regions irradiated by the laser spot were immobilized. As shown in Figure 5a, 5b and 5c, three microstructures were fabricated at 7.27 mW, 9.46 mW and 11.27 mW, respectively. It can be found that the microstructure fabricated at 7.27 mW has higher accuracy compared with those fabricated at 9.46 mW and 11.27 mW, demonstrating that the accuracy of microstructures is improved with decreasing laser power. Figure 5d is the side view of adenovirus fabricated at 8 mW. It was confirmed that the microstructure simulating morphology of adenovirus was precisely prepared, which originated from the high LSR.

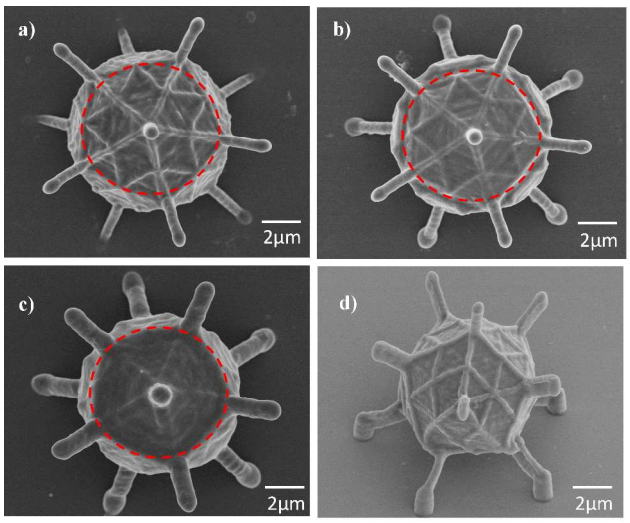

Fig. 5 SEM images of 3D hydrogels simulating the morphology of adenovirus. (a-c) the top view of 3D hydrogels fabricated at 7.27 mW, 9.46 mW and 11.27 mW, respectively. d) The side view of 3D hydrogels fabricated at 8 mW.

Conclusions

In summary, we have proposed a method to use highly sensitive initiator to improve the resolution of 3D hydrogels fabricated by TPP. The threshold energy of TPP was 6.29 mW for the self-assembled initiator of 2, 7-bis(2-(4-dimethylamino-phenyl)-vinyl)-anthraquinone and PF127. The lateral spatial resolution of 3D hydrogels was dramatically improved to 92 nm that can guarantee the processing accuracy of TPP microfabrication. Finally, the microstructure simulating the morphology of adenovirus was fabricated at the laser power near to the threshold energy of TPP. The proposed protocol for achieving 3D hydrogel with high spatial resolution would provide high potential for the molecule design of the high efficient initiators and the development of 3D arbitrary micro/nanostructures with precise configuration.

Acknowledgements

Authors thank the support of National Natural Science Foundation of China (31371014, 91323301, 51203111, 61205194, 61475164, 61275048 and 91123032) and Tianjin Natural Science Foundation (13JCYBJC16500).

Notes and references

[a]*School of Chemical Engineering and Technology, Tianjin University, Tianjin 300072, P. R.China.*
[b]*Laboratory of Organic NanoPhotonics and Key Laboratory of Functional Crystals and Laser Technology, Technical Institute of Physics and Chemistry, Chinese Academy of Sciences, No.29 Zhongguancun East Road, Beijing 100190, P. R. China.*
[c]*Chongqing Institute of Green and Intelligent Technology, Chinese Academy of Sciences, No.266 Fangzheng Ave, Shuitu technology development zone, Beibei District, Chongqing 400714, P. R. China.*
E-mail: jinfengxing@tju.edu.cn; zhengmeiling@mail.ipc.ac.cn; xmduan@mail.ipc.ac.cn

1. N. A. Peppas, J. Z. Hilt, A. Khademhosseini, R. Langer, *Adv. Mater.*, 2006, 18, 1345-1360.
2. J. Torgersen, X. H. Qin, Z. Q. Li, A. Ovsianikov, R. Liska, J. Stampfl, *Adv. Funct. Mater.*, 2013, 23, 4542-4554.
3. M. T. Raimondi, S. M. Eaton, M. M. Nava, M. Laganà, G. Cerullo, R. Osellame, *J. Appl. Biomater. Biomech.*, 2012, 10, 55-65.
4. K. M. Park, J. Yang, H. Jung, J. Yeom, J. S. Park, K. Park, A. S. Hoffman, S. K. Hahn, K. Kim, *ACS Nano*, 2012, 6, 2960-2968.
5. J. R. Xavier, T. Thakur, P. Desai, M. K. Jaiswal, N. Sears, E. Cosgriff-Hernandez, R. Kaunas, A. K. Gaharwar, *ACS Nano*, 2015, 9, 3109-3118.
6. Y. Xu, H. B. Sun, J. Y. Ye, S. Matsuo, H. Misawa, *J. Opt. Soc. Am. B* 2001, 18, 1084-1090.
7. X. G. Dai, W. Yang, E. Firlar, S. A. E. Marras, M. Libera, *Soft Matter,* 2012, 8, 3067-3076.
8. F. Quinonez, J. W. Menezes, L. Cescato, V. F. Rodriguez-Esquerre, H. Hernandez-Figueroa, and R. D. Mansano, *Opt. Express,* 2006, 14, 4873-4879.
9. S. W. Lee, K. S. Lee, J. Ahn, J. J. Lee, M. G. Kim, Y. B. Shin, *ACS Nano,* 2011, 5, 897-904.
10. S. Kawata, H. B. Sun, T. Tanaka, K. Takada, *Nature*, 2001, 412, 697-698.
11. Z. B. Sun, X. Z. Dong, W. Q. Chen, S. Nakanishi, X. M. Duan, S. Kawata, *Adv. Mater.* 2008, 20, 914-919.
12. W. K. Wang, Z. B. Sun, M. L. Zheng, X. Z. Dong, Z. S. Zhao, X. M. Duan, *J. Phys. Chem. C,* 2011, 115, 11275-11281.
13. J. F. Xing, M. L. Zheng, X. M. Duan, *Chem. Soc. Rev.*, 2015, 44, 5031-5039.
14. T. Watanabe, M. Akiyama, K. Totani, S. M. Kuebler, F. Stellacci, W. Wenseleers, K. Braun, S. R. Marder, J. W. Perry, *Adv. Funct. Mater.*, 2002, 12, 611-614.
15. A. Ovsianikov, M. Malinauskas, S. Schlie, B. Chichkov, S. Gittard, R. Narayan, M. Löbler, K. Sternberg, K.-P. Schmitz, A. Haverich, *Acta. Biomater.*, 2011, 7, 967-974.

16. A. Ovsianikov, V. Mironov, J. Stampfl, R. Liska, *Expert. Rev. Med. Devices*, 2012, 9, 613-633.
17. A. Ovsianikov, M. Gruene, M. Pflaum, L. Koch, F. Maiorana, M. Wilhelmi, A. Haverich, B. Chichkov, *Biofabrication*, 2010, 2, 014104.
18. Z. Xiong, M. L. Zheng, X. Z. Dong, W. Q. Chen, F. Jin, Z. S. Zhao, X. M. Duan, *Soft Matter*, 2011, 7, 10353-10359.
19. J. F. Xing,; J. H. Liu, T. B. Zhang, L. Zhang, M. L. Zheng, X. M. Duan, *J. Mater. Chem. B*, 2014, 2, 4318-4323.
20. J. C. Culver, J. C. Hoffmann, R. A. Poché, J. H. Slater, J. L. West, M. E. Dickinson, *Adv. Mater.*, 2012, 24, 2344-2348.
21. A. I. Ciuciu, P. J. Cywiński, *RSC Adv.*, 2014, 4, 45504-45516.
22. K. Takada, H. B. Sun, S. Kawata, *Appl. Phys. Lett.*, 2005, 86, 071122.
23. J. F. Xing, X. Z. Dong, W. Q. Chen, X. M. Duan, N. Takeyasu, T. Tanaka, S. Kawata, *Appl. Phys. Lett.*, 2007, 90, 131106.
24. X. Z. Dong, Z. S. Zhao, X. M. Duan, *Appl. Phys. Lett.*, 2008, 92, 091113.
25. L. Li, R. R. Gattass, E. Gershgoren, H. Hwang, J. T. Fourkas, *Science*, 2009, 324, 910-913.
26. D. F. Tan, Y. Li, F. J. Qi, H. Yang, Q. H. Gong, X. Z. Dong, X. M. Duan, *Appl. Phys. Lett.*, 2007, 90, 071106.
27. J. F. Xing, W. Q. Chen, X. Z. Dong, T. Tanaka, X. Y. Fang, X. M. Duan, S. Kawata, *J. Photoch. Photobio. A,* 2007, 189, 398-404.
28. J. Gu, W. Yulan, W. Q. Chen, X. Z. Dong, X. M. Duan, S. Kawata, *New J. Chem.*, 2007, 31, 63-68.
29. Y. C. Zheng, M. L. Zheng, S. Chen, Z. S. Zhao, X. M. Duan, *J. Mater. Chem. B*, 2014, 2, 2301-2310.
30. C. Xu, W. W. Webb, *J. Opt. Soc. Am. B,* 1996, 13, 481-491.
31. Y. Q. Tian, C. Chen, Y. Cheng, A. C. Young, N. M. Tucker, A. K.-Y. Jen, *Adv. Funct. Mater.*, 2007, 17, 1691-1697.
32. F. Jin, L. T. Shi, M. L. Zheng, X. Z. Dong, S. Chen, Z. S. Zhao, X. M. Duan, *J. Phys. Chem. C,* 2013, 117, 9463-9468.
33. D. Beljonne, J. L. Brédas, M. Cha, W. E. Torruellas, G. I. Stegeman, J. W. Hofstraat, W. H. G. Horsthuis, G. R. Möhlmann, *J. Chem. Phys.*, 1995, 103, 7834-7843.
34. O. K. Nag, R. R. Nayak, C. S. Lim, I. H. Kim, K. Kyhm, B. R. Cho, H. Y. Woo, *J. Phys. Chem. B*, 2010, 114, 9684-9690.
35. W. Saenger, T. Steiner, *Acta. Cryst. A*, 1998, 54, 798-805.
36. S. J. Jhaveri, J. D. McMullen, R. Sijbesma, L. S. Tan, W. Zipfel, C. K. Ober, *Chem. Mater.*, 2009, 21, 2003-2006.
37. J. Torgersen, A. Ovsianikov, V. Mironov, N. Pucher, X. Qin, Z. Li, K. Cicha, T. Machacek, R. Liska, V. Jantsch, J. Stampfl, *J. Biomed. Opt.*, 2012, 17,105008.